FLOOD FLOW SIMULATION IN LOW LAND AREAS BY TWO-DIMENSIONAL MODEL

Arvind Kumar GARG
CONSULTANT, Chuo fukken Consultants Co. Ltd., yodogawa-ku, Osaka 532
Yoshiaki IWASA
Professor, Dept of Civil Engg., Kyoto University, Kyoto 606.
Kazuya INOUE
Assoc. Professor, Dept of Civil Engg., Kyoto University, Kyoto 606.
Kiyoshi MATSUMOTO
CONSULTANT, Chuo fukken Consultants Co. Ltd., yodogawa-ku, Osaka 532

This paper presents a numerical simulation model of flood flow in low land areas. The application of the model is verified by checking the continuity equation at every computational time. Although there remains some points to be refined, this would be a promising method for the approach to the mitigation of flood hazards in low land areas.

Keywords : Flood flow, simulation, low land area, two-dimensinal model, drainage channel, drainage pump

1. INTRODUCTION

The low land areas or urban areas has been associated to our activity since the human birth and therefore have been developed in view of socio-economic, technical and cultural aspects. Thus the chances of potential losses in man's lives and property due to floods caused by heavy rainfalls have also been increased. The traditional methods of tackling floods are not feasible because they require a large amount of capital funds. One dimensional unsteady free surface flow equations are also not capable of yielding realistic predictions for water depth & discharge because of the problems in assessing the impacts of various activities of the inhabitants that are likely to alter the whole flood flow phenomena. So a two-dimensional model is formulated for the simulation of flood flow caused by heavy rainfalls over the ogura basin. The basin is located in the southern part of Kyoto and is a junction of two river, Kizu & Katsura to the main river of Uji(Yodo). To protect the area from flooding a pump is installed into the basin whose capacity is also decided into the present study. To have the sufficient water at the pump, a drainage channel is dug into the basin. Two cases for a drainage channel is considered:

Case 1: A channel of width 20m in the middle of the cells whose location is marked in Fig. (1) is assumed. The figure also shows the position of two barrier banks in the basin.

Case 2: A straight channel of uniform bottom elevation of width 231m (cell northward length) and upto distance of about 3km from the pump is assumed.

The fundamental equations consist of continuity and momentum equations in two space dimensions (x, y). A staggered finite difference scheme of multi-levels (leap-frog type) is used for the solution. The more details of the method are available from Garg(1988).

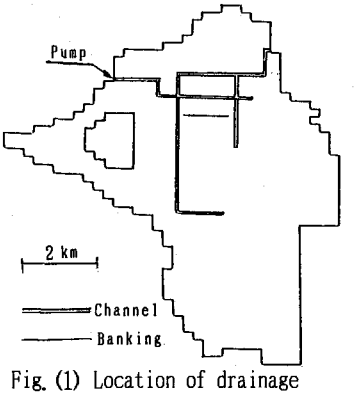

Fig. (1) Location of drainage channel & banking in case 1.

2. MATHEMATICAL MODEL

2.1 Mean flow equations:

The plane one-layered mathematical model equations are derived from integrating the basic Navier-Stockes equations over the water depth of control volume shown in Fig. (2). The depth-averaged two-dimensional model equations which can realize the actual simulation of excess rainfall over a basin read as follows

$$\frac{\partial h}{\partial t}+\frac{\partial M}{\partial x}+\frac{\partial N}{\partial y}=r_e \qquad (1)$$

$$\frac{\partial M}{\partial t}+\frac{\partial}{\partial x}(uM)+\frac{\partial}{\partial y}(vM)=-gh\frac{\partial H}{\partial x}-\frac{\tau_x(b)}{\rho} \qquad (2)$$

$$\frac{\partial N}{\partial t}+\frac{\partial}{\partial y}(uN)+\frac{\partial}{\partial y}(vN)=-gh\frac{\partial H}{\partial y}-\frac{\tau_y(b)}{\rho} \qquad (3)$$

where H: water stage, M: the flow flux in the x-direction(uh), N: the flow flux in the y-direction (vh), r_e :effective rainfall, h: water depth, g: acceleration of gravity, t: time u, v: velocity component in the x and y-direction respectively, x, y: distance in the east and northward directions, ρ: water density, τ_x (b), τ_y (b): bottom shear stresses on the bed in the x and y-directions respectively.

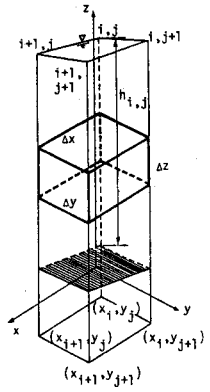

Fig. (2) Control volume

The main assumptions in deriving the eqns. (1)-(3) are

(i) The hydrostatic vertical pressure distribution.

(ii) Horizontal exchange of momentum due to turbulent motions is ignored, on the assumption that it is much less significant than other processes such as bottom and surface friction.

(iii) The boussinesq approximation of much smaller density variation in a water body than the density itself is introduced; therefor constant density is used in the momentum equations.

(iv) The effects due to Coriolis force and wind shear stress at the surface is neglected.

The bottom shear stresses depend upon the characteristics of the flow and on the vertical velocity distribution, particularly in the zone near the bottom, which is in turn related to the horizontal pressure gradients, The bottom shear stress on the bed is expressed by

$$\tau_{x,y}(b)=\rho g n^2(u,v)(u^2+v^2)^{1/2}/h^{1/3} \qquad (4)$$

The non-linear bottom friction can produce strong effects at large velocities and small depths, since it has a quadratic dependence on velocity and an inverse quadratic dependence on depth.

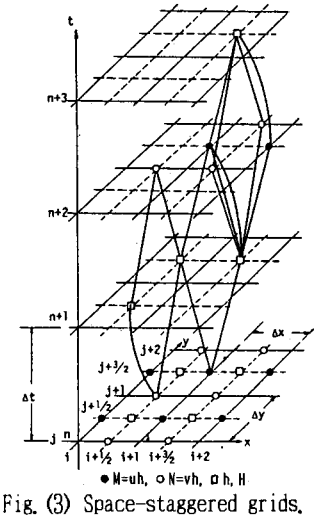

Fig. (3) Space-staggered grids.

2.2 *Finite difference representation of model equations:*

Numerical scheme used in this paper is similar to that reported earlier by Iwasa and Inoue (1982). Using the space-staggered grids in Fig. (3) in explicit scheme and defining the variables on the grids shown in Fig. (4), eqns. (1)-(3) are transformed into finite difference form as

Equation of Continuity:

$$\frac{h^{n+3}_{i+1/2,\,j+1/2}-h^{n+1}_{i+1/2,\,j+1/2}}{2\Delta t}+\frac{M^{n+2}_{i+1,\,j+1/2}-M^{n+2}_{i,\,j+1/2}}{\Delta x}+\frac{N^{n+2}_{i+1/2,\,j+1}-N^{n+2}_{i+1/2,\,j}}{\Delta y}$$

$$=r^{n}_{e\,i+1/2,\,j+1/2} \qquad (5)$$

Momentum equation without non-linear convective terms in the x-direction

$$\frac{M^{n+2}_{i,\,j+1/2}-M^{n}_{i,\,j+1/2}}{2\Delta t}=-g\frac{(h^{n+1}_{i-1/2,\,j+1/2}+h^{n+1}_{i+1/2,\,j+1/2})(H^{n+1}_{i+1/2,\,j+1/2}-H^{n+1}_{i-1/2,\,j+1/2})}{2\Delta x}$$

$$-gn^2_{i,\,j+1/2}\frac{(M^{n}_{i,\,j+1/2}+M^{n+2}_{i,\,j+1/2})^2\sqrt{(u^{n}_{i,\,j+1/2})^2+(v^{n}_{i,\,j+1/2})^2}}{2[(h^{n+1}_{i-1/2,\,j+1/2}+h^{n+1}_{i+1/2,\,j+1/2})/2]^{4/3}} \qquad (6)$$

where,

$$u^{n}_{i,\,j+1/2} = 2M^{n}_{i,\,j+1/2} \,/\, (h^{n+1}_{i-1/2,\,j+1/2} + h^{n+1}_{i+1/2,\,j+1/2}) \tag{7}$$

$$v^{n}_{i,\,j+1/2} = \frac{(N^{n}_{i-1/2,\,j} + N^{n}_{i+1/2,\,j} + N^{n}_{i+1/2,\,j+1} + N^{n}_{i-1/2,\,j+1})}{2\,(h^{n+1}_{i-1/2,\,j+1/2} + h^{n+1}_{i+1/2,\,j+1/2})} \tag{8}$$

Momentum equation in the y-direction in also expressed in the same way as eqn. (6) in which,

$$u^{n}_{i+1/2,\,j} = \frac{(M^{n}_{i,\,j-1/2} + M^{n}_{i+1,\,j-1/2} + M^{n}_{i+1,\,j+1/2} + M^{n}_{i,\,j+1/2})}{2\,(h^{n+1}_{i+1/2,\,j-1/2} + h^{n+1}_{i+1/2,\,j+1/2})} \tag{9}$$

$$v^{n}_{i+1/2,\,j} = \frac{2N^{n}_{i+1/2,\,j}}{(h^{n+1}_{i+1/2,\,j-1/2} + h^{n+1}_{i+1/2,\,j+1/2})} \tag{10}$$

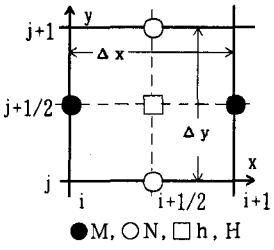

Fig. (4) Variables location on grids

Non-linear terms expression:

Non-linear Convective terms with respect to the geometric scale are expressed in backward difference as

$$\frac{\partial}{\partial x}(uM) = \frac{u^{*}_{i+1/2,\,j+1/2}\,M^{*}_{i+a,\,j+1/2} - u^{*}_{i-1/2,\,j+1/2}\,M^{*}_{i-1+b,\,j+1/2}}{\Delta x} \tag{11}$$

$$u^{*}_{i+1/2,\,j+1/2}\,M^{*}_{i+a,\,j+1/2} = \begin{cases} u^{*}_{i+1/2,\,j+1/2}\,M^{*}_{i,\,j+1/2} & u^{*}_{i+1/2,\,j+1/2} \geq 0 \\ u^{*}_{i+1/2,\,j+1/2}\,M^{*}_{i+1/2,\,j+1/2} & u^{*}_{i+1/2,\,j+1/2} < 0 \end{cases} \tag{12}$$

$$u^{*}_{i,\,j+1/2} = \frac{2M^{*}_{i,\,j+1/2}}{(h^{*}_{i-1/2,\,j+1/2} + h^{*}_{i+1/2,\,j+1/2})} \tag{13}$$

$$u^{*}_{i+1/2,\,j+1/2} = \frac{(u^{*}_{i,\,j+1/2} + u^{*}_{i+1,\,j+1/2})}{2} \tag{14}$$

The solution at $t = (n+2)\Delta t$ is obtained by using the solution at $t = n\,\Delta t$ and $(n+1)\Delta t$; first M^{n+2} and N^{n+2} is obtained by using eqns. (6)-(8) with eqns. (11)-(14) and the similar equations of y-direction and then h^{n+3} is calculated by using eqn. (5).

The boundary conditions used in numerical analysis are in the following:

(i) At the solid boundary like banking, hillsides and similar ones $M = N = 0$ and $h = 0$

(ii) At the pumping station for drainage, the pump operation policy is defined and is transformed into the flow flux.

(iii) If the water depth at higher elevation cell is less than ε (say .001m) at the preceding time, t, then the in-and outflow fluxes from the higher elevation cell are assumed zero.

(iv) The computed flow flux is replaced by 0 at the cell where the estimated depth of water is less than ε.

(v) The negative depth, if computed, is replaced by 0.

(vi) Non-linear terms with respect to temporal scale are estimated by two values at $t = (n-2)\Delta t$ and $t = n\,\Delta t$ which are

$$u^{*} = (u^{n-2} + u^{n})/2, \quad M^{*} = (M^{n-2} + M^{n})/2, \quad h^{*} = (h^{n-1} + h^{n+1})/2,$$

(vii) Two types of exchange relationship between cells may be possible which are

(1) the weir type links which is possible when there is a local obstacles such as dikes or embankments and roads.

(2) the step-down or step-up type links when there is no local obstacles.

(1) the weir type links shown in Fig. (5) exists in the flow flux (M) in the x-direction where

$H^{n+1}_{i-1/2,\,j+1/2} > H^{n+1}_{i+1/2,\,j+1/2}$ and

$H^{n+1}_{i-1/2,\,j+1/2} > H_b$.

Defining

$h_1 = H^{n+1}_{i-1/2,\,j+1/2} - H_b$ and

$h_2 = H_{i-1/2,\,j+1/2}^{n+1} - H_b$,

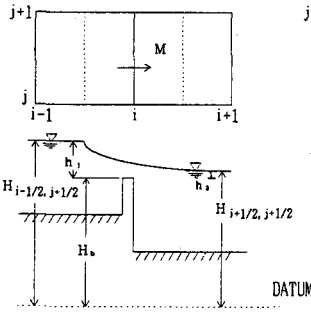

Fig. (5) Weir-type links between cells.

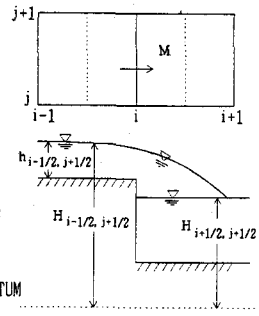

Fig. (6) Step-down type links between cells.

two cases are possible which are calculated in similar way as described by Cunge(1975)as

(a) when $h_2/h_1 \leqq 2/3$ (free-flow condition)

$$M^{n+2}_{i,\,j+1/2} = \mu_1 h_1 \sqrt{2gh_1} \qquad (15)$$

(b) when $h_2/h_1 > 2/3$ (submerged condition)

$$M^{n+2}_{i,\,j+1/2} = \mu_2 h_2 \sqrt{2g(h_1 - h_2)} \qquad (16)$$

where μ_1 and μ_2 are the coefficients which have the value equal to 0.35 and 0.91 respectively. The opposit case is dealt in the same way with negative sign for flow-flux.

Similarly, the flow-flux(N) in the y-direction is calculated when the above type of links exist between the cells in the y-direction.

(2) Step down type link shown in Fig. (6) exists in the flow-flux (M) in the x-direction and is calculated as

$$M^{n+2}_{i,\,j+1/2} = c h_{i-1/2,\,j+1/2} \sqrt{g h_{i-1/2,\,j+1/2}} \qquad (17)$$

where c is the coefficient equal to $(2/3)^{3/2} = 0.544$.

The step-up type links is dealt in the same way with negative sign for the flow-flux. Similarly, the flow-flux (N) in the y-direction is calculated when the above type of links exist between the cells in the y-direction.

TIME (hr)	VCHK	
	CASE 1	CASE 2
6	1.00000	1.00032
12	1.00000	1.00040
18	1.00000	1.00068
24	1.00000	1.00102
30	1.00000	1.00141
33	1.00000	1.00156
50	1.00000	1.00214
60	1.00000	1.00224
VCHK = (STORAGE+OUTFLOW)/INFLOW		

Table 1. Result of Continuity check

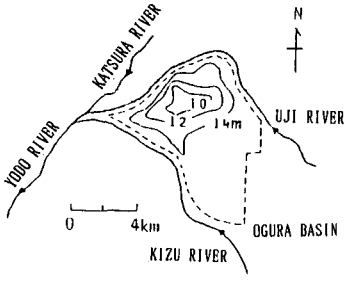

Fig. (7) Topographical map of Concerned area

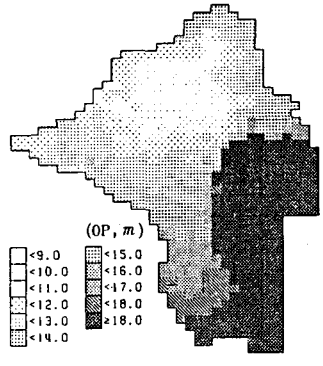

Fig. (8) Contour map

3. INFORMATION USED IN NUMERICAL ANALYSIS

(i) Ground levels ; Fig. (7) shows the topographical map of the the study basin. The contour map of the reclaimed basin in Fig. (8) gives the ground levels. The lowest part of the basin runs towards the north-west.

(ii) Cells ; The eastward cell length, Δx is 285.44m and the northward one, Δy is 231.0m.

(iii) Roughness ; The manning roughness coefficient used are

$n = 0.025$ for farmlands
$n = 0.040$ for populated area
$n = 0.060$ for mountains & hillside area

(iv) Initial conditions ; At $t = 0$,
$M = N = 0$, $h = 0$

(v) The time steps of computation is $\Delta t = 20$sec.

(vi) Effective rainfall is assumed to be uniformly distributed throughout the basin. The rainfall pattern is shown in Fig. (9).

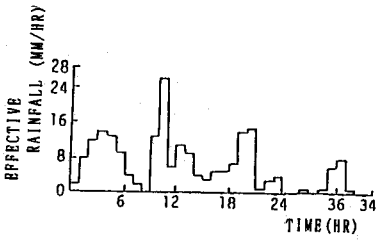

Fig. (9) Effective rainfall pattern

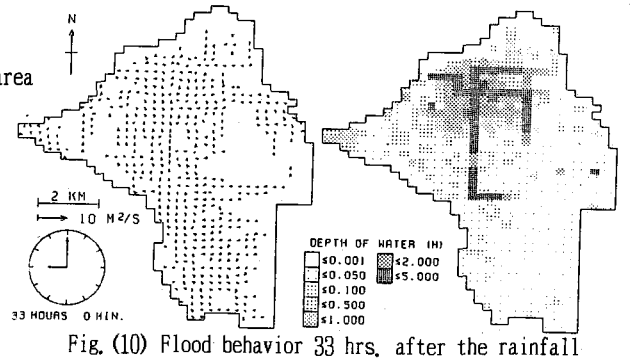

Fig. (10) Flood behavior 33 hrs. after the rainfall start in case 1

4. RESULTS AND CONCLUSIONS

(i) To verify the model, the continuty equation is checked at every computational time. The results are shown in Table 1 at a few computational times.

(ii) To decide the pump capacity, pumps of different capacity are used. And it is found that a pump of capacity $50m^3/s$ best fit to drain the water from this low land area.

(iii) Influential differences of the drainage systems and without drainage system on the overland flow in view of hydraulics are shown in Figs. (10)-(12).

(iv) The drainage channel considered in case 2 is found to be more effective than in case 1. It can be seen from Figs. (13)-(14). and Table 2. It may be because of low conveyance velocity of the area. In case 2 the pump operates at its full capacity after 13 hrs of rainfall and to drain most of the water from the basin it needs approximately 32 more hours after the rainfall stops. The results presented herein, however, indicate that the present model has performed sufficient well in this low land basin that it can, and should, now be applied to other low land basins.

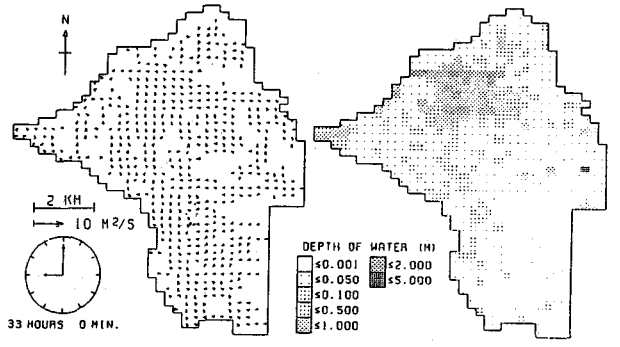

Fig. (11) Flood behavior 33 hrs. after the rainfall start in case 2

CASE	AFTER 22 hrs OF PEAK RAINFALL	
	STORAGE (M^3)	OUTFLOW (M^3)
1	10.346×10^6	0.4360×10^6
2	6.571×10^6	4.1947×10^6
WITHOUT DRAINAGE SYSTEM	10.782×10^6	—
CASE 2 : AFTER 28 hrs OF RAINFALL STOP STORAGE : 2.8547×10^6 OUTFLOW : 7.9037×10^6		

Table 2. Computed result of storage & outlow

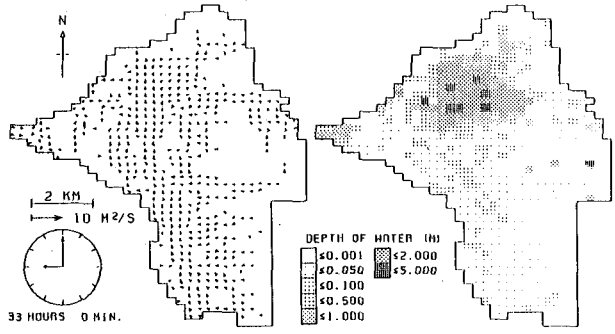

Fig. (12) Flood behavior 33 hrs. after the rainfall start in case of without drainage.

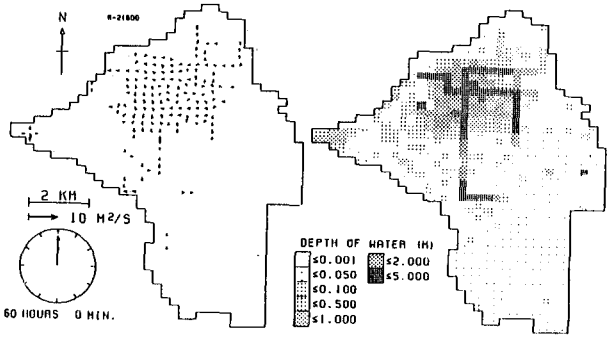

Fig. (13) Flood behavior 60 hrs. after the rainfall start in case 1.

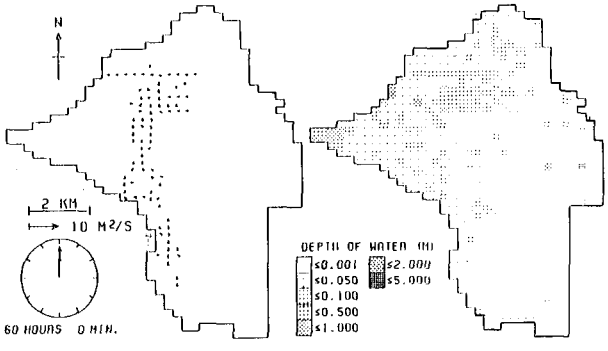

Fig. (14) Flood behavior 60 hrs. after the rainfall start in case 2.

5. References :

1. Cunge, J. A., and Verwey, A. (1975), Two-dimensional modelling of flood plains in unsteady flow in open channels (K. Mahmood & V. Yevjevich eds.)
2. Garg, A. K. (1988), Ph. D. Thesis, Dept. of Civil Engg., Kyoto University, Kyoto Japan
3. Iwasa, Y. and Inoue, K., Mathematical Simulation of channel and overland flood flows in view of flood disaster engineerig, Journal of Natural Disaster Science, Vol. 4, Number 1, pp. 1-30.